Neuron
Article

Bidirectional Regulation of Dendritic Voltage-Gated Potassium Channels by the Fragile X Mental Retardation Protein

Hye Young Lee,[1] Woo-Ping Ge,[1] Wendy Huang,[1] Ye He,[1] Gordon X. Wang,[2] Ashley Rowson-Baldwin,[1] Stephen J. Smith,[2] Yuh Nung Jan,[1] and Lily Yeh Jan[1,*]
[1]Howard Hughes Medical Institute Departments of Physiology, Biochemistry, and Biophysics, University of California, San Francisco, CA 94158, USA
[2]Department of Molecular and Cellular Physiology, Stanford University, Stanford, CA 94305, USA
*Correspondence: lily.jan@ucsf.edu
DOI 10.1016/j.neuron.2011.09.033

SUMMARY

How transmitter receptors modulate neuronal signaling by regulating voltage-gated ion channel expression remains an open question. Here we report dendritic localization of mRNA of Kv4.2 voltage-gated potassium channel, which regulates synaptic plasticity, and its local translational regulation by fragile X mental retardation protein (FMRP) linked to fragile X syndrome (FXS), the most common heritable mental retardation. FMRP suppression of Kv4.2 is revealed by elevation of Kv4.2 in neurons from *fmr1* knockout (KO) mice and in neurons expressing Kv4.2-3′UTR that binds FMRP. Moreover, treating hippocampal slices from *fmr1* KO mice with Kv4 channel blocker restores long-term potentiation induced by moderate stimuli. Surprisingly, recovery of Kv4.2 after *N*-methyl-D-aspartate receptor (NMDAR)-induced degradation also requires FMRP, likely due to NMDAR-induced FMRP dephosphorylation, which turns off FMRP suppression of Kv4.2. Our study of FMRP regulation of Kv4.2 deepens our knowledge of NMDAR signaling and reveals a FMRP target of potential relevance to FXS.

INTRODUCTION

Mammalian central neurons rely on the dynamic interplay between transmitter receptors and voltage-gated ion channels on their dendrites for signal processing. For example, the A-type voltage-gated K^+ channels (I_A) on the dendrites of CA1 hippocampal pyramidal neurons regulate neuronal signaling by filtering fast synaptic potentials and regulating action potential back propagation, synaptic integration and long-term potentiation (LTP) (Kim and Hoffman, 2008). This I_A derives primarily from Kv4.2 (Birnbaum et al., 2004; Kim et al., 2007; Chen et al., 2006). Enriched on the spines of CA1 pyramidal neurons, Kv4.2 is under the regulation of synaptic activity and it in turn contributes to the regulation of synaptic plasticity (Kim et al., 2007; Jung et al., 2008). Whether Kv4.2 mRNA is targeted to dendrites to present the opportunity of local regulation by synaptic activity is an open question.

How Kv4.2 regulation may help neurons to stay within the dynamic range of synaptic plasticity is another open question. Whereas the rapid downregulation of Kv4.2 upon *N*-methyl-D-aspartate receptor (NMDAR) activation due to its internalization and degradation (Kim et al., 2007; Lei et al., 2008; Lei et al., 2010) provides positive feedback to enhance excitation, the dendritic potassium channel level has to quickly recover after a barrage of synaptic activities, given that loss of Kv4.2 function causes enhanced induction of LTP (Chen et al., 2006) while increasing Kv4.2 expression abolishes the ability to induce LTP (Jung et al., 2008). Because alteration of Kv4.2 levels is associated with epilepsy and possibly Alzheimer's disease (Birnbaum et al., 2004) and the *KCND2* gene coding for Kv4.2 is near rearrangement breakpoints in autism patients (Scherer et al., 2003), better understanding of the dynamic regulation of Kv4.2 by synaptic activities will help future analyses of the contribution of this potassium channel to neuronal signaling as well as its involvement in neurological and mental disorders.

The importance of local synthesis of dendritic proteins in synaptic plasticity (Kelleher et al., 2004; Sutton and Schuman, 2005) has stimulated recent studies on trafficking of neuronal RNA granules (Kiebler and Bassell, 2006), regulation of local synthesis of synaptic proteins (Schuman et al., 2006; Sutton and Schuman, 2005) and mRNA transport (Sossin and DesGroseillers, 2006). One of the RNA binding proteins implicated is the fragile X mental retardation protein (FMRP) linked to Fragile X syndrome (FXS), the most common heritable mental retardation that is often associated with autism (Bagni and Greenough, 2005). Multiple symptoms of FXS patients including the altered spine morphology (Greenough et al., 2001; Hinton et al., 1991; Irwin et al., 2001) is recapitulated in *fmr1* knockout (KO) mice (Comery et al., 1997; Nimchinsky et al., 2001), which also display compromised learning, abnormal behavior and altered synaptic plasticity (Penagarikano et al., 2007). This mouse model of FXS is therefore a suitable system for examining FMRP contribution to synaptic regulation of local translation.

FMRP can bind to its target mRNA directly or indirectly (Bagni and Greenough, 2005). It has multiple RNA-binding domains and may regulate mRNA localization (Dictenberg et al., 2008), mRNA

stability (Zalfa et al., 2007) or mRNA translation (Muddashetty et al., 2007; Zalfa et al., 2003) in central neurons (Bassell and Warren, 2008). Because FMRP is localized to dendrites and spines (Antar et al., 2004), it could regulate local protein synthesis underlying spine development and synaptic plasticity (Antar and Bassell, 2003; Bagni and Greenough, 2005). The mGluR (metabotropic glutamate receptor) theory of FXS posits that FMRP normally acts downstream of Group1 mGluR as a repressor of translation; in the absence of FMRP, there is runaway protein synthesis that leads to exaggerated long-term depression (LTD) (Bear et al., 2004). Notably, LTP induced by moderate theta burst stimulation (TBS) is also impaired in the CA1 hippocampal field of *fmr1* KO mice (Lauterborn et al., 2007), raising the question as to how FMRP might affect synaptic plasticity.

For FMRP to be involved in dynamic regulation of dendritic mRNA, its grip on translational repression should be under synaptic regulation as well. How can FMRP repression be relieved? Phosphorylation of FMRP is a candidate mechanism (Ceman et al., 2003; Narayanan et al., 2007, 2008). Given that expression of FMRP with intact phosphorylation site causes an increase of stalled polyribosomes, dephosphorylation of FMRP may be associated with the release of polyribosomes from the stalled state (Ceman et al., 2003). Consistent with this scenario, Group1 mGluR activation causes transient dephosphorylation of FMRP (Narayanan et al., 2007, 2008), which may allow rapid mRNA regulation by FMRP. Whereas the involvement of mGluR in FMRP regulation has been investigated extensively, potential roles of other transmitter receptors in FMRP regulation still await analyses (Bassell and Warren, 2008), notwithstanding recent studies implicating NMDAR in FMRP regulation (Edbauer et al., 2010; Gabel et al., 2004b; Pilpel et al., 2009).

In this study, we show dendritic localization of Kv4.2 mRNA and FMRP suppression of local translation of the Dendra-Kv4.2 fusion protein in isolated dendrites. We demonstrate FMRP binding to the 3′UTR of Kv4.2 mRNA (Kv4.2-3′UTR) and identify domains of both FMRP and Kv4.2-3′UTR involved in their interaction, which likely contributes to FMRP suppression of Kv4.2 because expression of Kv4.2-3′UTR increases Kv4.2 level in neurons. Indeed, our analyses of *fmr1* KO mice reveal that FMRP is important for Kv4.2 suppression in vivo. We further show that the deficit in LTP induction can be rescued by reducing Kv4 channel activity in hippocampal slices from *fmr1* KO mice.

Unexpectedly, we found that NMDAR activation not only transiently reduces Kv4.2 protein level due to degradation as reported previously, but also increases Kv4.2 protein production in an FMRP-dependent process likely involving Kv4.2-3′UTR. We discovered that NMDAR activation causes dephosphorylation of mTOR and the downstream S6 kinase S6K1 as well as the ribosomal protein S6 and FMRP—both substrates of S6K1. We then expressed mutant FMRP in cultured hippocampal neurons from *fmr1* KO mice lacking FMRP, and found that S499D but not S499A mutant FMRP retains the ability to dampen the exuberant Kv4.2 surface expression on the dendrites of hippocampal neurons from *fmr1* KO mice, as well as the ability to suppress translation associated with Kv4.2-3′UTR. Taken together, our study identifies Kv4.2 mRNA as a target of FMRP; whereas FMRP suppresses Kv4.2 in basal conditions, FMRP suppression is relieved by dephosphorylation upon NMDAR activation to increase Kv4.2 expression following synaptic activity, thereby maintaining neurons within the dynamic range of synaptic plasticity.

RESULTS

Kv4.2 mRNA Localizes to the Dendrites of Mouse Hippocampal Neurons

Given the involvement of dendritic Kv4.2 potassium channels in the regulation of synaptic plasticity, it is important to determine whether Kv4.2 mRNA resides in the dendrites. We could detect endogenous Kv4.2 mRNA in hippocampal neurons after 14 days in vitro (DIV14) by fluorescence in situ hybridization (FISH) using an antisense probe against the 3′UTR region of Kv4.2 mRNA; the control sense probe did not show any specific mRNA staining (see Figure S1 available online). We found Kv4.2 mRNA in cell bodies and along dendrites in a punctate distribution (Figure 1B). Moreover, Kv4.2 mRNA colocalized with dendritic marker MAP2 but not with axonal marker tau1 (Figure 1C). Moreover, we found dendritic localization of Kv4.2 mRNA in the CA1 dendritic field of the hippocampus (Figure 1A).

3′UTR of Kv4.2 mRNA (Kv4.2-3′UTR) Is Important for Dendritic Targeting

To test whether the 3′UTR of Kv4.2 mRNA, which is relatively long (2.5 kb) with its first 1.5 kb of sequences highly conserved between human and rodents (Figure S2), can mediate dendritic targeting, we used the MS2 system for tracking the subcellular localization of RNAs (Fusco et al., 2003). We fused Kv4.2-S.3′UTR (sense) or Kv4.3-A.S.3′UTR (antisense) to MS2BS(6X) containing six tandem RNA hairpins that are binding sites for the RNA binding protein MS2 (Figure 2A). Cotransfection of DIV10–12 hippocampal neurons with MS2BS(6X)-Kv4.2-S.3′UTR and MS2-GFP-NLS (nuclear localization signal) made it possible to delineate the distribution of chimeric RNA containing MS2 binding sites (MS2BS) and Kv4.2-3′UTR via its association with GFP-tagged MS2. The control RNA containing only MS2 binding sites but no 3′UTR appeared exclusively inside the nucleus in all of the transfected neurons (Figure 2B) due to the presence of NLS in the GFP-tagged MS2 fusion protein. The control MS2BS(6X)-Kv4.2-A.S.3′UTR also yielded similar nuclear localization (Figure 2B). In contrast, MS2BS(6X)-Kv4.2-S.3′UTR appeared in the cytoplasm and also entered the dendrites, giving rise to a punctate pattern (Figure 2B), similar to the appearance of the MS2BS(6X)-Arc-S.3′UTR (Figure S3). Thus, the 3′UTR of Kv4.2 mRNA is sufficient for dendritic targeting.

FMRP Colocalizes with Kv4.2 mRNA in Neuronal Dendrites and Binds to Kv4.2-3′UTR

Because FMRP is known to be present in multiple RNA-containing granules (Sossin and DesGroseillers, 2006), we examined neurons double-labeled for FMRP and Kv4.2 mRNA and found partial overlap of Kv4.2 mRNA and FMRP granules in proximal and distal dendrites (Figure 3B), similar to the overlapping distribution of FMRP and Arc mRNA, a target of FMRP

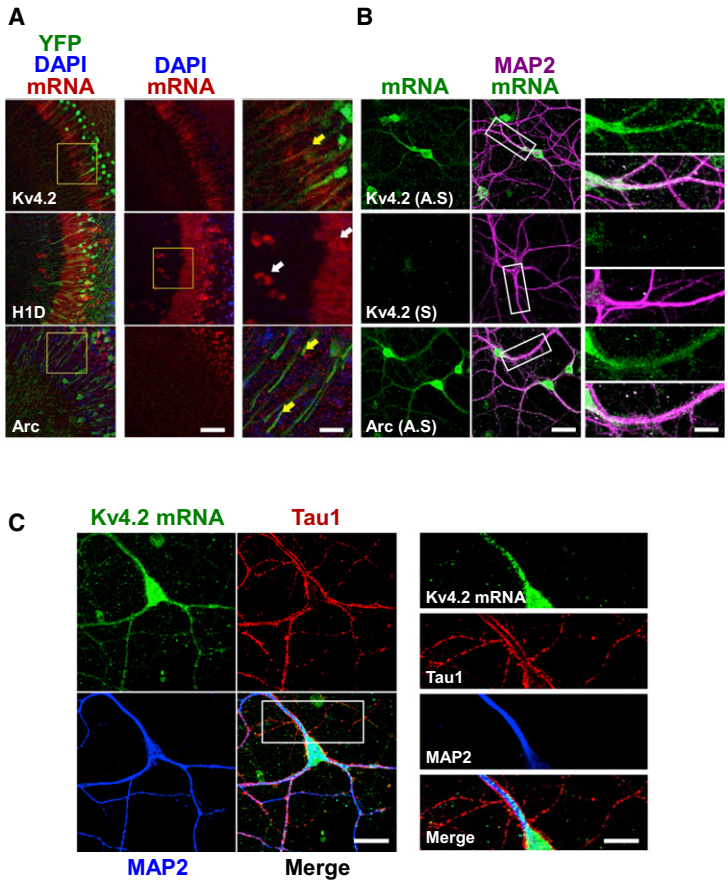

Figure 1. Kv4.2 mRNA Localizes in Dendrites of Mouse Hippocampus and Cultured Hippocampal Neurons

(A) Kv4.2 (top), histone 1D (H1D) (middle), or Arc mRNA (bottom) (red) in the CA1 region of mouse hippocampus revealed by FISH using antisense probe to the 3′UTR together with nuclear marker DAPI (blue); scale bar represents 100 μm. Boxed regions are shown at high magnification on the right; scale bar represents 30 μm. Arrows point to examples of soma labeled with H1D mRNA (white) or a couple of the numerous cases in which Kv4.2 or Arc mRNA signal colocalizes with YFP-positive (green) dendrites.

(B) Kv4.2 or Arc mRNA (green) in MAP2-positive (magenta) dendrites of mouse hippocampal neurons (DIV14) revealed by FISH using an antisense (top) or a sense (middle) probe against Kv4.2-3′UTR, or an antisense probe against Arc-3′UTR (bottom); scale bar represents 30 μm. Boxed dendrites in left panels are shown at high magnification on the right; scale bar represents 10 μm. See Figure S1 for more examples.

(C) Kv4.2 mRNA (green) revealed by FISH using an antisense probe against Kv4.2-3′UTR, localizes in MAP2-positive (blue) dendrites but not tau1-positive (red) axons in DIV14 mouse hippocampal neurons; scale bar represents 20 μm. Boxed region in left panels is shown at high magnification on the right; scale bar represents 10 μm.

(Figure S4A). We further show that Kv4.2 mRNA coimmunoprecipitated with FMRP from the adult mouse brain lysate (Figure 3A), similar to the coimmunoprecipitation of FMRP with PSD-95 mRNA, another target of FMRP. Finally, we monitored concerted movements of FMRP and Kv4.2-3′UTR by live imaging of neurons expressing MS2-GFP-NLS and MS2BS(6X)-Kv4.2-S.3′UTR together with fluorescently tagged FMRP following NMDAR activation, which enhanced the movement of these granules (Figure 3C). Taken together, these findings indicate that FMRP is associated with Kv4.2 mRNA in neuronal dendrites.

We then tested for binding of FMRP to the 3′UTR of Kv4.2 mRNA, because in silico analysis of this region has revealed the presence of U-rich stretches (Figure S2), a sequence motif for RNA binding to FMRP (Chen et al., 2003). By using streptavidin-beads to pull down proteins from brain lysates bound to biotinylated Kv4.2-3′UTR, we found FMRP binding of Kv4.2-S.3′UTR (Figure 3D) at a level comparable to that of Arc-3′UTR or PSD-95-3′UTR (Figures S4B and S5A). This binding is specific to FMRP because Kv4.2-3′UTR showed no association with the RNA-binding protein Staufen or non-RNA binding proteins such as mTOR, dynamin 1, and actin (Figure S5A). Furthermore, the binding is direct as evident from the interaction between bacterially expressed and purified FMRP and Kv4.2-S.3′UTR, at a level comparable to the interaction between FMRP and PSD-95-3′UTR (Figure 3E; Figure S5B). This binding is specific because FMRP binds Kv4.2-3′UTR but not GFP mRNA or Kv4.2-A.S.3′UTR (Figures 3D and 3E).

Next, we examined the three domains of FMRP individually. Only the C-terminal domain of FMRP was specifically pulled-down with Kv4.2-3′UTR (Figure 3F). This domain contains an RGG box known to have an affinity for mRNAs. We then tested five RNA fragments that together encompass the entire 3′UTR of the mouse Kv4.2 mRNA, and found only fragment 2 and fragment 5 that contain U-rich sequences associated with the purified FMRP C-terminal domain (Figure 3G). Notably, fragment 2 includes an evolutionarily conserved U-rich sequence (Figure S2). Taken together, these studies show that the direct interaction between FMRP and Kv4.2-3′UTR is likely evolutionarily conserved.

FMRP Is Not Required for Kv4.2 mRNA Dendritic Targeting or Stability

We found the Kv4.2 mRNA level in the hippocampus of *fmr1* KO mice was similar to that in wild-type (WT) mice (Figure 4A). We confirmed the gene targeting using primers that amplify exon 5 (or exon 1) of the *fmr1* (or Kv4.2) gene that is interrupted by the neomycin resistance selection marker gene in the *fmr1* (or Kv4.2) KO mice (Figure 4A); using other primers we found that these KO mice have some remnant, genetically altered, transcripts. Using the MS2 system to track the subcellular localization of MS2BS(6X)-Kv4.2-S.3′UTR in hippocampal neurons with or without FMRP, we found similar dendritic targeting (Figure 4B), indicating that FMRP is not required for dendritic targeting of Kv4.2-3′UTR. We further performed quantitative FISH analysis using an antisense probe against Kv4.2-3′UTR and examined the distribution of endogenous Kv4.2 mRNA in dendrites. We found similar dendritic localization and punctate pattern of Kv4.2 mRNA in WT and *fmr1* KO neurons (Figure 4C), and similar Kv4.2 mRNA levels along dendrites of neurons with or

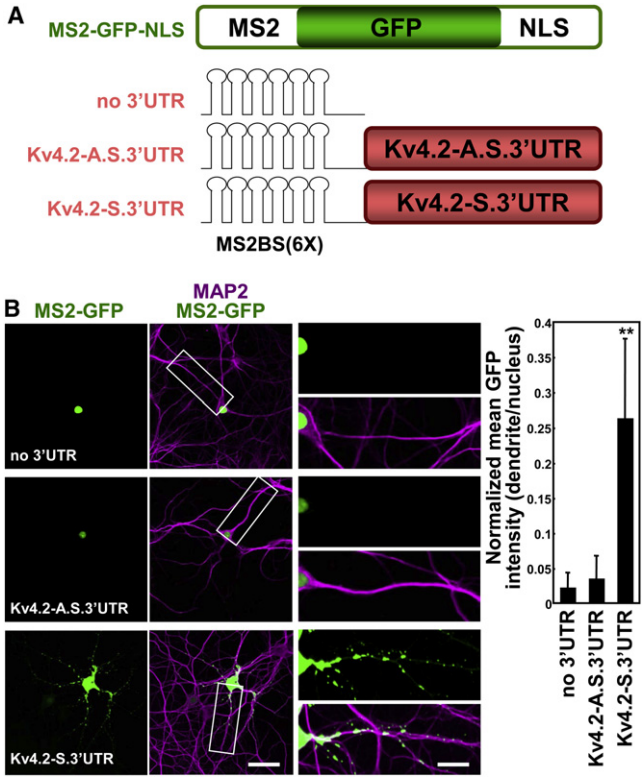

Figure 2. Kv4.2-3′UTR Is Important for Dendritic Targeting in Mouse Hippocampal Neurons

(A) Schematic depiction of MS2 constructs for visualization of Kv4.2-3′UTR (antisense or sense).

(B) Left: mouse hippocampal neurons (DIV14) cotransfected with MS2-GFP-NLS (green) and MS2BS(6X)-no 3′UTR (top), MS2BS(6X)-Kv4.2-antisense 3′UTR (middle), or MS2BS(6X)-Kv4.2-sense 3′UTR (bottom) are shown with MAP2 staining for dendrites (magenta); scale bar represents 30 μm. Boxed dendrites in left panels are shown at high magnification on the right; scale bar represents 10 μm. Right: mean GFP intensity of dendrites normalized to that of the nucleus of the same neurons (mean ± SD; n = 7, 8, and 8 dendrites each from four neurons transfected with MS2BS(6X)-no 3′UTR, Kv4.2-A.S.3′UTR, or Kv4.2-S.3′UTR, respectively. **$p < 0.01$ as compared with MS2BS(6X)-no 3′UTR, Student's unpaired t test). See Figure S2 for sequence similarity between human, rat, and mouse Kv4.2-3′UTR, and Figure S3 for dendritic targeting of Arc-S.3′UTR as a positive control.

without FMRP (Figure 4C). Taken together, these results suggest that FMRP is not essential for Kv4.2 mRNA dendritic targeting or stability in basal conditions.

FMRP Suppresses Kv4.2 Protein Levels in Hippocampal Neuronal Dendrites

To test for FMRP regulation of Kv4.2 protein expression we compared Kv4.2 levels in the hippocampus from adult WT and *fmr1* mutant mice, using Kv4.2 KO mice as control for Kv4.2 antibody specificity (Figure 5A and 5B). We found ~1.5–2-fold increase of Kv4.2 immunoreactivity in the CA1 dendritic field of the hippocampus from 3-week-old and 2-month-old *fmr1* KO mice (Figure 5A), and a similar increase of Kv4.2 protein levels in the hippocampus from adult *fmr1* KO mice (Figure 5B).

Next, we performed surface biotinylation on cultured hippocampal neurons and used actin both as loading control and to confirm that our biotinylation protocol results in biotinylation of surface but not cytosolic proteins. We found higher surface as well as total Kv4.2 levels in DIV14 hippocampal neurons without FMRP (Figure 5C). Using antibody against an extracellular epitope of Kv4.2 for immunostaining of unpermeabilized DIV14 hippocampal neurons, we found higher levels of Kv4.2 on the dendritic surface of neurons without FMRP (Figure 5D). Because both total Kv4.2 protein levels and the surface expression of Kv4.2 on dendrites are elevated in the absence of FMRP whereas the relative proportions of surface and total Kv4.2 protein levels were not significantly altered, these findings indicate that FMRP suppresses Kv4.2 production.

To test whether FMRP binding to Kv4.2-3′UTR could suppress protein production, we performed an in vitro translation assay using *Renilla* luciferase transcript fused to Kv4.2-3′UTR together with firefly luciferase transcript for normalization, and included either purified GST as control or purified GST-mouse full-length FMRP, and nuclease-treated rabbit reticulocyte lysates. We found that FMRP suppressed Kv4.2-3′UTR-dependent translation by 60% ($p < 0.001$, $n = 4$) (Figure 5F). Moreover, expression of MS2BS(6X)-Kv4.2-S.3′UTR but not MS2BS(6X) alone led to an increase of surface Kv4.2 expression (Figure 5E), indicating that FMRP suppression of Kv4.2 is relieved by disruption of FMRP interaction with the 3′UTR of Kv4.2 mRNA via MS2BS(6X)-Kv4.2-S.3′UTR. Taken together, these findings support the notion that FMRP suppression of Kv4.2 protein expression in neuronal dendrites is due to translational repression via its association with Kv4.2-3′UTR.

FMRP Suppresses Local Translation of Dendra-Kv4.2 in Isolated Dendrites

To look for evidence of Kv4.2 local translation in the dendrites of cultured hippocampal neurons, we expressed Dendra-Kv4.2 in these neurons, severed a dendrite via UV illumination from the 2-photon microscope, photo-converted the existing Dendra-Kv4.2 from green to red and then monitored the appearance of newly synthesized green Dendra-Kv4.2 in the dendrite separated from the neuronal soma (Figure 5G). We found a nearly 2-fold increase of Dendra-Kv4.2 local translation in isolated dendrites from hippocampal neurons without FMRP (Figure 5G), indicating that Kv4.2 local translation is likely under the control of FMRP.

LTP Restoration by Reducing Kv4 Activity in Hippocampal Slice from *fmr1* KO Mice

The hippocampus-dependent learning deficits of *fmr1* KO mice are associated with an inability of moderate levels of theta burst stimulation to induce LTP as evident from field recording of the excitatory postsynaptic potential (fEPSP) (Lauterborn et al., 2007). As reported, five theta bursts of Schaffer collaterals stimulation induced LTP in hippocampal slices from WT mice (Figure 6A) but not *fmr1* KO mice (Figure 6B) of postnatal day 14–21, whereas ten theta bursts were sufficient to induce LTP in both. Using the heteropodatoxin HpTx2 from a family of spider toxins specific for blocking Kv4 channels (Ramakers and Storm, 2002; Sanguinetti et al., 1997), we found HpTx2

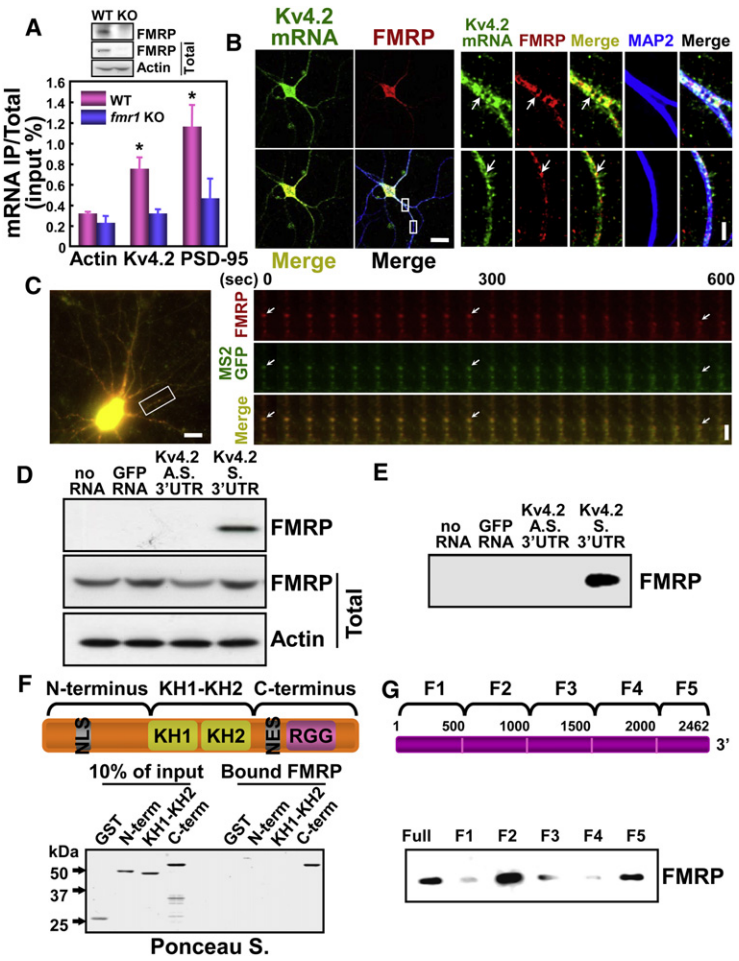

Figure 3. Kv4.2-3′UTR Interacts with FMRP

(A) Top: immunoprecipitation of FMRP from adult mouse brain lysates of WT or *fmr1* KO mice. Immunoprecipitated FMRP was immunoblotted with FMRP antibody (top). We immunoblotted 10% input (Total) of brain lysates (30 μg) with FMRP or actin antibody. Bottom: quantitative measurement of actin mRNA, Kv4.2 mRNA, or PSD-95 mRNA coimmunoprecipitated with FMRP from brain lysates of WT or *fmr1* KO mice. As described in Supplemental Experimental Procedures, complexes were immunoprecipitated with FMRP antibody and analyzed via qRT-PCR. The input % was calculated by dividing the signal for coimmunoprecipitated mRNA using FMRP antibody by the signal for input (Total) (mean ± SD; n = 3 for both WT and *fmr1* KO mice, *$p < 0.05$ as compared with *fmr1* KO, Student's unpaired t test).

(B) Kv4.2 mRNA (green) revealed by FISH using an antisense probe against Kv4.2-3′UTR, colocalizes with FMRP (red) in MAP2-positive (blue) dendrites in DIV14 mouse hippocampal neurons. Merged images of Kv4.2 mRNA and FMRP are shown in yellow and merged images of Kv4.2 mRNA, FMRP, and MAP2 are shown in white; scale bar represents 20 μm. Boxed dendrites in left panels are shown at high magnification on the right; scale bar represents 5 μm.

(C) Time lapse live imaging of neurons transfected with mCherry-FMRP (red), MS2BS(6X)-Kv4.2-sense 3′UTR and MS2-GFP-NLS (green) with indicated time after 100 μM NMDA treatment. Boxed dendrite in the left panel (0 s; scale bar represents 20 μm) is shown at high magnification on the right (0–600 s; scale bar represents 5 μm). Merged images of FMRP (top) and Kv4.2-3′UTR (middle) are shown in yellow (bottom).

(D) Binding assay performed with biotinylated RNA (no RNA, GFP cRNA, Kv4.2-antisense 3′UTR, or Kv4.2-sense 3′UTR) and mouse brain lysates, as described in Supplemental Experimental Procedures. Complexes were pulled-down with streptavidin-beads and immunoblotted with FMRP antibody (top). We immunoblotted 10% input (Total) of brain lysates (30 μg) with FMRP or actin antibody.

(E) Binding assay performed with biotinylated RNA (no RNA, GFP cRNA, Kv4.2-antisense 3′UTR, or Kv4.2-sense 3′UTR) and purified GST-mouse full-length FMRP, as described in Supplemental Experimental Procedures. Complexes were pulled-down with streptavidin-beads and immunoblotted with FMRP antibody.

(F) Top: schematic depiction of FMRP fragments (N terminus, KH1-KH2, and C terminus) used for binding assay with biotinylated Kv4.2-3′UTR. Bottom: binding assay performed with biotinylated Kv4.2-3′UTR and purified GST or GST-FMRP fragments. We subjected 10% input of proteins and complexes pulled down with streptavidin-beads to SDS-PAGE followed by Ponceau staining.

(G) Top: schematic depiction of Kv4.2-3′UTR fragments (F1, F2, F3, F4, and F5) used for binding assay with purified C-terminal domain of FMRP. Bottom: binding of purified GST-C-terminal domain of FMRP to biotinylated Kv4.2-3′UTR or some of its fragments. Complexes were pulled-down with streptavidin-beads and immunoblotted with GST antibody. Data shown in (D-G) represent three independent experiments each. See Figure S4 for similar experiments with Arc-3′UTR as positive controls and Figure S5 for Kv4.2-3′UTR coimmunoprecipitation with FMRP or phospho-S6 but not the RNA-binding protein Staufen, with PSD-95-3′UTR as a positive control for coimmunoprecipitation and binding assays.

dose-dependently restored LTP induction by five theta burst stimuli to slices from *fmr1* KO mice but did not significantly alter LTP of control WT slices (Figures 6C and 6D). It thus appears that hippocampal neurons from *fmr1* KO mice have excessive Kv4 channel activity due to the lack of FMRP suppression, thereby compromising synaptic plasticity.

NMDAR Activation Induces Kv4.2 Translation

We next test whether NMDAR regulates Kv4.2 protein levels in DIV14–21 hippocampal neurons, and found that 5 min treatment with 100 μM NMDA induced first a robust decrease of Kv4.2 levels, which then quickly recovered 15 min after washing out NMDA (total time elapsed from the start of the NMDA treatment is 20 min) (Figure 7A). The NMDA-induced reduction of total Kv4.2 levels is attributed to degradation (Lei et al., 2008) and is dependent on calpain activity (Lei et al., 2010). We therefore pretreated neurons with a mixture of calpain inhibitors (MDL+ALLN) for 15 min before applying NMDA for 5 min, and waited for another 15 min after washing out of NMDA to monitor NMDAR-mediated Kv4.2 regulation without the confounding effects of Kv4.2 degradation. In the presence of calpain inhibitors, NMDA treatment no longer caused a reduction of Kv4.2 levels, instead the Kv4.2 protein levels progressively increased by ~2–2.5-fold ($p < 0.01$, n = 4) following NMDAR activation (Figure 7B; Figure S6). These experiments reveal that NMDAR activation causes upregulation of Kv4.2 production concurrent with Kv4.2 degradation, to fine tune Kv4.2 levels following NMDAR activation and allow their restoration in due course.

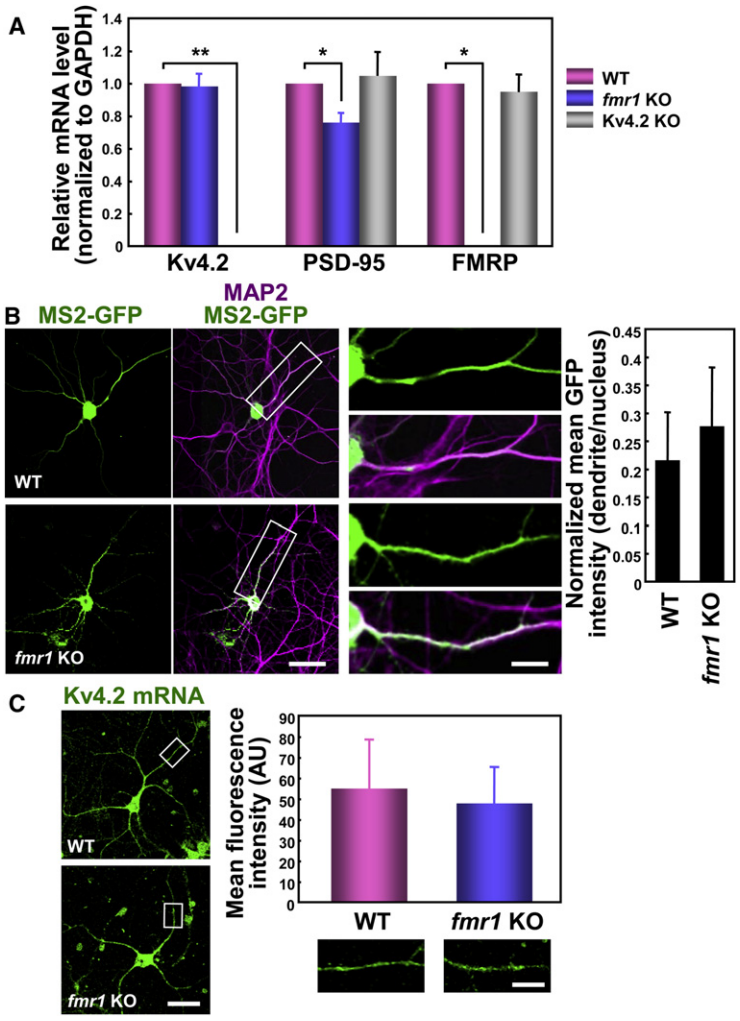

Figure 4. Kv4.2 mRNA Dendritic Targeting or Stability Is Not Affected by FMRP in Mouse Hippocampal Neurons

(A) Relative mRNA level (normalized to GAPDH mRNA) of Kv4.2, PSD-95, or FMRP in hippocampus from WT, *fmr1* KO, or Kv4.2 KO mice determined by qRT-PCR analysis (WT level was set as 1, mean ± SD; n = 3 each for WT, *fmr1* KO, or Kv4.2 KO mice, *p < 0.5, **p < 0.01 as compared with WT, Student's unpaired t test).

(B) Left: cotransfected hippocampal neurons (DIV14) from WT (top) or *fmr1* KO (bottom) mice with MS2BS(6X)-Kv4.2-3′UTR and MS2-GFP-NLS (green) are shown with MAP2 staining (magenta); scale bar represents 30 μm. Boxed dendrites in left panels are shown at high magnification on the right; scale bar represents 10 μm. Right: mean GFP intensity of dendrites normalized to that of the nucleus in neurons transfected with MS2BS(6X)-Kv4.2-sense 3′UTR from WT or *fmr1* KO neurons (mean ± SD; n = 7 for WT, n = 6 for *fmr1* KO, p > 0.1 as compared with WT, Student's unpaired t test).

(C) Left: Kv4.2 mRNA in dendrites of hippocampal neurons (DIV14) from WT (top) or *fmr1* KO (bottom) mice revealed by FISH using an antisense probe against Kv4.2-3′UTR; scale bar represents 30 μm. Right: mean fluorescence intensity of dendritic Kv4.2 mRNA (top) from WT or *fmr1* KO hippocampal neurons (mean ± SD; n = 12 for WT, n = 13 for *fmr1* KO, p > 0.1 as compared with WT, Student's unpaired t test). Boxed dendrites in left panels are shown at high magnification (bottom); scale bar represents 5 μm.

We also performed a dual-luciferase reporter assay to look into the effect of NMDAR activation on translation associated with Kv4.2-3′UTR, and found that Kv4.2-3′UTR-dependent translation of luciferase increased shortly after NMDA treatment (Figure 7C), reaching a plateau 30 min after NMDA treatment before finally decreasing several hours later. Taken together, our results show that NMDAR activation induces upregulation of Kv4.2 expression in hippocampal neurons likely in a process mediated by Kv4.2-3′UTR.

FMRP Is Required for NMDAR-Induced Upregulation of Kv4.2

Having found that NMDAR activation causes upregulation of Kv4.2 expression, we next asked whether this regulation involves FMRP. Western analyses revealed that WT neurons showed robust recovery of Kv4.2 within 15 min, after the NMDAR-induced degradation caused a ~2-fold reduction ($p < 0.01$, n = 3) of Kv4.2 protein level. In contrast, the Kv4.2 levels of neurons from *fmr1* KO mice remained reduced after NMDAR activation and showed no recovery (Figure 7D).

Next, we asked whether FMRP is required for NMDAR-induced upregulation of translation that is dependent on Kv4.2-3′UTR. Using the dual-luciferase reporter assay, we found that Kv4.2-3′UTR-dependent production of luciferase increased in response to NMDAR activation in WT neurons but not in neurons from *fmr1* KO mice (Figure 7E). Given that in *fmr1* KO mice there is excess basal Kv4.2 expression due to a lack of FMRP suppression of Kv4.2, the requirement of FMRP for NMDAR-induced upregulation of Kv4.2 production as well as Kv4.2-3′UTR-dependent translation raises the question whether this synaptic regulation could be due to a relief of FMRP suppression of Kv4.2.

NMDAR Activation Mediates Dephosphorylation of FMRP through PP1

How might FMRP suppression of Kv4.2 be turned off? FMRP may repress translation of its target mRNA by stalling ribosomes, which could be diminished by synaptic activity and dephosphorylation of FMRP (Ceman et al., 2003; Narayanan et al., 2007, 2008). To test whether NMDAR activation might turn off FMRP repression of Kv4.2, we examined FMRP phosphorylation at Serine 499 preceding the RGG box, a posttranslational modification known to take place within 2–4 hr of FMRP synthesis (Ceman et al., 2003). Remarkably, we found rapid dephosphorylation of FMRP within 5 min exposure of DIV14–21 hippocampal neurons to NMDA (Figure 8A), accompanied with rapid dephosphorylation of mTOR, S6 kinase (S6K1), and S6 (Figure 8A) whereas the total protein levels of these proteins were unchanged. Given that the ribosomal S6 kinase S6K1 is the primary kinase for FMRP phosphorylation at S499 (Narayanan et al., 2008), FMRP

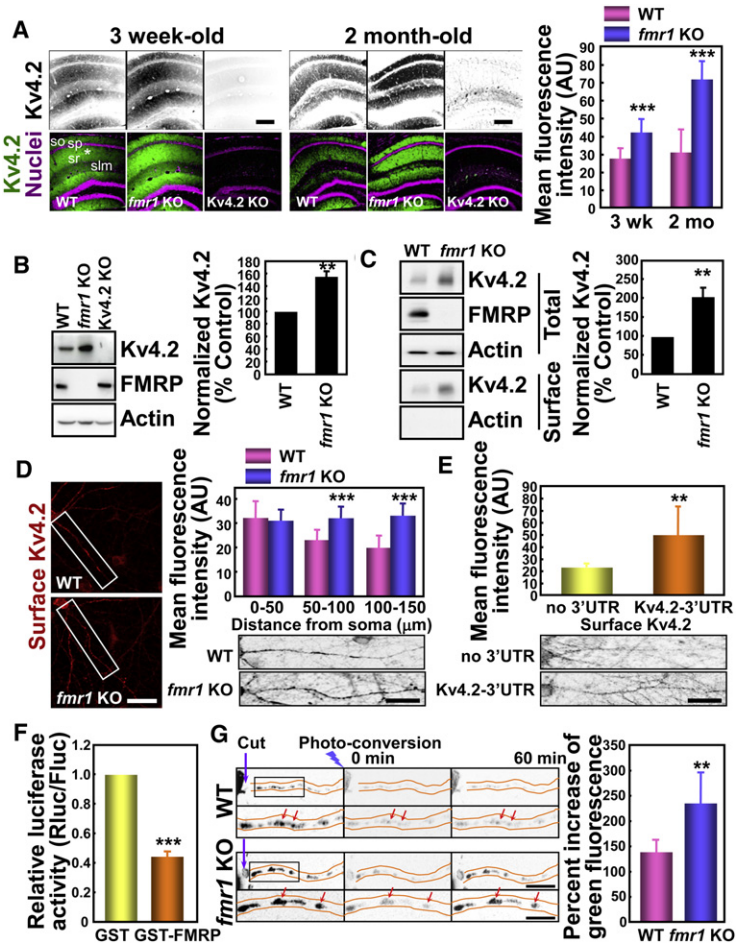

Figure 5. FMRP Suppresses Kv4.2 Protein Levels in Hippocampal Neuronal Dendrites and Local Protein Translation of Kv4.2

(A) Left: Kv4.2 distribution (black in single images [top]; green in merged images [bottom]) in hippocampal slices from 3-week-old or 2-month-old WT (left), *fmr1* KO (middle), or Kv4.2 KO (right) mice stained with DAPI (magenta); scale bar represents 400 μm. Right: mean fluorescence intensity of Kv4.2 in CA1 dendritic field of mouse hippocampal slices (marked with *, area quantified: 10,184 pixels, mean ± SD; n = 15 for WT and n = 53 for *fmr1* KO that are 3 weeks old, n = 20 for WT and n = 22 for *fmr1* KO that are 2 months old, ***p < 0.001 as compared with WT of the same age, Student's unpaired t test).

(B) Left: Kv4.2 levels in hippocampus from WT, *fmr1* KO, or Kv4.2 KO mice. Mouse hippocampus lysates were immunoblotted with Kv4.2, FRMP or actin antibody. Right: Kv4.2 levels normalized with actin levels (% control to WT, mean ± SD; n = 4 for both WT and *fmr1* KO, **p < 0.01 as compared with WT, Student's paired t test).

(C) Left: surface biotinylation of hippocampal neurons (DIV14) from WT or *fmr1* KO mice, as described in Supplemental Experimental Procedures. Top: 10% input (Total) of cell lysates (30 μg) was immunoblotted with Kv4.2, FMRP, or actin antibody. Bottom: biotinylated samples (Surface) were immunoblotted with Kv4.2 or actin antibody. Right: surface Kv4.2 levels normalized with Total actin levels (% control to WT, mean ± SD; n = 4 for both WT and *fmr1* KO, **p < 0.01 as compared with WT, Student's paired t test).

(D) Left: Kv4.2 surface staining of hippocampal neurons (DIV14) from WT or *fmr1* KO mice, as described in Supplemental Experimental Procedures; scale bar represents 30 μm. Right: mean fluorescence intensity of surface Kv4.2 in dendrites (top) from WT or *fmr1* KO hippocampal neurons (mean ± SD; n = 10, 15, and 13 for WT dendrites at 0–50, 50–100, and 100–150 μm from the soma, respectively; n = 17, 20, and 18 for *fmr1* KO neuronal dendrites at 0–50, 50–100, and 100–150 μm from the soma, respectively, ***p < 0.001 as compared with WT, Student's unpaired t test). Boxed dendrites in left panels are shown at high magnification (bottom); scale bar represents 20 μm.

(E) Mean fluorescence intensity of surface Kv4.2 in dendrites (top) from hippocampal neurons transfected with no 3′UTR or Kv4.2-3′UTR (mean ± SD; n = 7 dendrites for no 3′UTR, n = 8 dendrites for Kv4.2-3′UTR, **p < 0.01 as compared with no 3′UTR, Student's unpaired t test). Dendrites are shown at high magnification (bottom); scale bar represents 20 μm.

(F) In vitro translation assay with *Renilla* luciferase-Kv4.2-3′UTR in presence of GST or GST-FMRP, normalized with firefly luciferase activity (Rluc/Fluc), as described in Supplemental Experimental Procedures (GST control was normalized as 1, mean ± SD; n = 4, ***p < 0.001 as compared with GST, Student's paired t test).

(G) Left: live imaging of Dendra-Kv4.2 expressing mouse hippocampal neurons from WT or *fmr1* KO mice before, immediately after (0 min), and 60 min after UV exposure, as described in Supplemental Experimental Procedures. Representative grayscale images of green fluorescence in neurons (top); scale bar represents 10 μm. Dendrite in boxed region with arrow pointing to a single Dendra-Kv4.2 puncta (bottom); scale bar represents 5 μm. Right: normalized newly synthesized Dendra-Kv4.2 (green fluorescence pixel intensity) in individual puncta (mean ± SD; n = 6 dendrites for both WT and *fmr1* KO, **p < 0.01 as compared with WT, Student's unpaired t test).

dephosphorylation is likely a consequence of the inhibition of mTOR pathway shortly after NMDAR activation. As expected, treatment with the mTOR inhibitor rapamycin also resulted in FMRP dephosphorylation (Figure S7).

We then tested the effects of phosphatase inhibitors. We treated neurons with 20 nM okadaic acid or 50 nM fostriecin to inhibit PP2A, 1 μM okadaic acid to inhibit PP1 and PP2A, or 10 μM cyclosporine A to inhibit PP2B/calcineurin. Whereas dephosphorylation of FMRP and mTOR was unaffected by treatment with 20 nM okadaic acid or 50 nM fostriecin, which inhibit PP2A, or the PP2B inhibitor cyclosporine A at 10 μM as compared with the DMSO carrier control, 1 μM okadaic acid greatly reduced dephosphorylation of both mTOR and FMRP following NMDAR activation (Figure 8B; Figure S8). These experiments reveal that PP1 is required for NMDAR-induced dephosphorylation of mTOR and its downstream effectors including S6 and FMRP. Thus, the signaling pathway for NMDAR-induced upregulation of Kv4.2 likely involves PP1 activation by NMDAR (Chung et al., 2009), leading to dephosphorylation of mTOR. This inhibition of the mTOR pathway then results in dephosphorylation of substrates of S6K1 downstream of mTOR, such as FMRP.

Phosphorylation-Dependent FMRP Suppression of Kv4.2

To test whether regulation of FMRP phosphorylation at S499 might account for the regulation of Kv4.2-3′UTR-dependent translation, we compared the WT form of FMRP with mutant

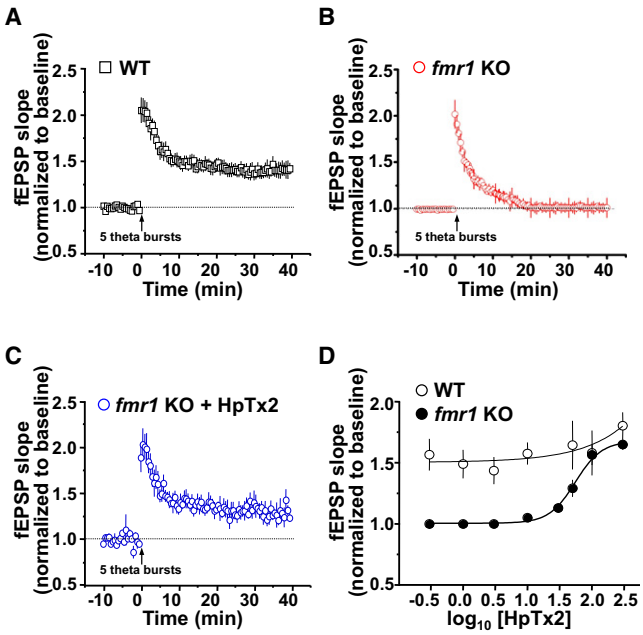

Figure 6. LTP Restoration by Reducing Kv4 Activity in Hippocampal Slice from *fmr1* KO Mice

(A–C) fEPSPs to single pulses of stimulation of Schaffer collaterals were collected from the dendritic field of CA1 neurons for 40 min in WT (A; n = 16 slices from eight animals), *fmr1* KO (B; n = 27 slices from three animals), or *fmr1* KO mice in presence of 50 nM HpTx2 (C; n = 8 slices from four animals). A single train of five theta bursts was delivered (arrow, time 0) to the Schaffer collaterals and the group data (mean ± SEM) are expressed as the percentage of mean fEPSP slopes recorded during the baseline (pre-theta burst) period. (D) Different concentrations of HpTx2 were used to enhance LTP in WT or *fmr1* KO mice: 0.3, 1, 3, 10, 30, 50, 100, 300 nM (WT mice: n = 3 from one animal for 0.3 nM, n = 6 from two animals each for 1, 3, and 100 nM, n = 7 from three animals for 10 nM, n = 4 from two animals for 30 nM, n = 5 from two animals for 300 nM, *fmr1* KO mice: n = 3 from one animal each for 0.3, 1, 3, 10, and 30 nM, n = 8 from four animals for 50 nM, n = 7 from four animals for 100 nM, n = 4 from two animals for 300 nM). Group data (mean ± SEM) are expressed as the percentage of mean fEPSP slopes recorded during the baseline (pre-theta burst) period.

FMRP with S499 replaced by Alanine (S499A) or Aspartate (S499D) (Ceman et al., 2003), and performed a dual-luciferase reporter assay by cotransfecting HEK293 cells with *Renilla* luciferase-Kv4.2-3′UTR together with firefly luciferase, plus GFP-tagged FMRP (WT, S499A, S499D), or GFP alone as control. In contrast to the suppression of Kv4.2-3′UTR-dependent luciferase production by FMRP-WT and FMRP-S499D (Figure 8C), FMRP-S499A showed much less suppression (Figure 8C). Thus, FMRP phosphorylation at S499 appears to be crucial for FMRP suppression of translation associated with Kv4.2-3′UTR.

To test whether regulation of FMRP phosphorylation affects Kv4.2 channel density on neuronal dendrites, we transfected cultured hippocampal neurons from *fmr1* KO mice with GFP-tagged FMRP (WT, S499A, S499D), or GFP alone as control, and used antibody against extracellular epitope of Kv4.2 to assess its surface expression level. In control experiments involving transfecting hippocampal neurons from WT or *fmr1* KO mice with GFP, we found higher levels of surface expression of Kv4.2 on the dendrites of neurons from *fmr1* KO mice (Figure 8D). By introducing WT or mutant FMRP into hippocampal neurons from *fmr1* KO mice, we found that neurons expressing FMRP-WT or FMRP-S499D had similar levels of Kv4.2 surface expression whereas neurons expressing FMRP-S499A had significantly increased Kv4.2 protein levels on the surface of their dendrites (Figure 8D), indicating that the S499D but not S499A mutant form of FMRP retains the ability to suppress Kv4.2. Taken together, our results suggest Kv4.2-3′UTR-dependent protein synthesis as well as Kv4.2 channel density on neuronal dendrites depends on the status of FMRP phosphorylation.

DISCUSSION

The Dendritic Voltage-Gated Potassium Channel Kv4.2 as a Target of FMRP

This study provides evidence for dendritic targeting of mRNA of the Kv4.2 dendritic voltage-gated potassium channel that is important for controlling dendritic excitability and synaptic plasticity. FMRP suppresses Kv4.2 expression in basal conditions, and is also involved in NMDAR-mediated Kv4.2 upregulation due to its dephosphorylation. Our study thus defines a signaling pathway linking FMRP with dendritic Kv4.2 regulation by synaptic activity, and provides a lead for consideration regarding the etiology of FXS.

In addition to the interaction with FMRP for translation suppression, Kv4.2-3′UTR also mediates dendritic targeting (Jo et al., 2010) and increases steady state levels of mRNA. Taken together with the previous report on local translation of Kv1.1 mRNA in dendrites (Raab-Graham et al., 2006), voltage-gated ion channels now join the rank of postsynaptic scaffolding proteins such as PSD-95 and SAPAPs, activity-dependent synaptic proteins such as CaMKIIα, Arc, and MAP1b, and ligand-activated ion channels such as GluR1/2 and $GABA_AR\delta$ (Bassell and Warren, 2008) as dendritic proteins with their mRNAs localized in neuronal dendrites and under the regulation of synaptic activity.

FMRP Regulation of Kv4.2 Production and Synaptic Plasticity

FXS, the most common heritable mental retardation often associated with autism, is caused by the loss of FMRP function (Bagni and Greenough, 2005). Our finding of Kv4.2 mRNA association with FMRP in neuronal dendrites and direct binding of FMRP to Kv4.2-3′UTR led us to discover that Kv4.2 is under the control of FMRP. Whereas loss of FMRP resulted in no significant changes in Kv4.2 mRNA level or dendritic localization, it caused a dramatic increase of total Kv4.2 levels in the CA1 dendritic field of the hippocampus and in cultured hippocampal neurons from *fmr1* KO mice. Similar elevation of Kv4.2 levels was also found for surface expression of Kv4.2, especially on distal dendrites, revealing FMRP suppression of Kv4.2 in vivo.

Whereas we found elevated Kv4.2 in the hippocampal dendritic field of 3-week-old as well as 2-month-old *fmr1* KO mice (Figure 5A), a recent study reports Kv4.2 levels are reduced in *fmr1* KO mice (Gross et al., 2011), however, this conclusion is based on Kv4.2 immunostaining that shows a different pattern from the documented Kv4.2 expression in stratum radiatum

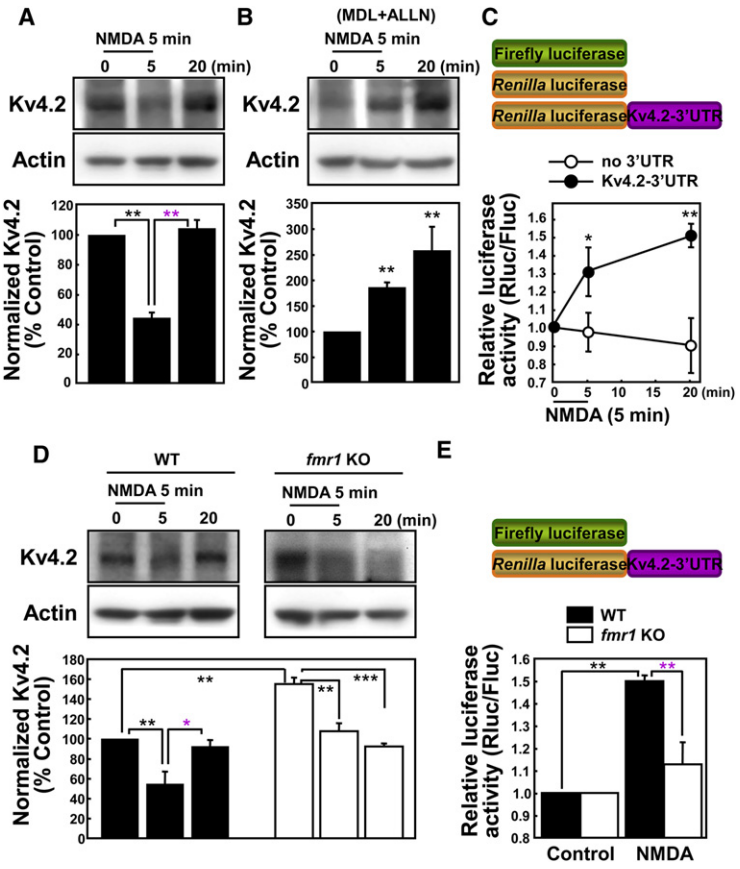

Figure 7. FMRP Is Required For NMDAR-Induced Upregulation of Kv4.2

(A and B) Top: mouse hippocampal neurons (DIV14–21) were treated with 100 μM NMDA, as described in Experimental Procedures without (A) or with pretreatment of 20 μM MDL and 25 μM ALLN for 15 min (B). Cell lysates were immunoblotted with Kv4.2 or actin antibody. Bottom: Kv4.2 levels normalized with actin levels (% control to not-treated cells, mean ± SD; n = 4 for both untreated and pretreated with MDL + ALLN, $^{**}p < 0.01$ as compared with not-treated cells (black) or 5 min NMDA-treated cells (magenta), Student's paired t test).

(C) Top: schematic depiction of luciferase constructs used for luciferase reporter assay. Bottom: *Renilla* luciferase activity normalized with firefly luciferase activity (Rluc/Fluc) in mouse hippocampal neurons (DIV14) upon NMDA treatment (not-treated cells were normalized as 1, mean ± SD; n = 3, $^{*}p < 0.05$, $^{**}p < 0.01$ as compared with not-treated cells, Student's paired t test).

(D) Top: hippocampal neurons (DIV14–21) from WT or *fmr1* KO mice were treated with 100 μM NMDA, as described in Experimental Procedures. Cell lysates were immunoblotted with Kv4.2 or actin antibody. Bottom: Kv4.2 levels normalized with actin levels (% control to WT not-treated cells, mean ± SD; n = 3, $^{*}p < 0.05$, $^{**}p < 0.01$, $^{***}p < 0.001$ as compared with not-treated cells (black) or 5 min NMDA-treated cells (magenta), Student's paired t test).

(E) Top: schematic depiction of luciferase constructs used for luciferase reporter assay. Bottom: *Renilla* luciferase activity normalized with firefly luciferase activity (Rluc/Fluc) in hippocampal neurons (DIV14) from WT or *fmr1* KO mice, compared between not-treated cells (Control) and 15 min after 5 min NMDA treatment cells (not-treated cells were normalized as 1, mean ± SD; n = 4, $^{**}p < 0.01$ as compared with not-treated cells (black) or WT (magenta), Student's paired t test). See Figure S6 for lack of NMDAR-induced Kv4.2 upregulation following pretreatment with calpain inhibitors of neurons from *fmr1* KO mice.

but low in stratum lacunosum moleculare (Menegola and Trimmer, 2006) thus raising question about the specificity of the immunostaining. This study also reports that GFP-Kv4.2 3′ UTR is associated with mCherry-FMRP but not mCherry-RGG or other FMRP fragments that contain one or both RNA-binding domains (Gross et al., 2011). In contrast, we found direct binding of Kv4.2 3′UTR to FMRP as well as its RGG-containing C-terminal domain (Figures 3E–3G).

Not only is FMRP required for suppression of dendritic Kv4.2, it is also essential for NMDAR-induced Kv4.2 protein production that enables Kv4.2 level to fully recover after its degradation and downregulation induced by NMDAR activation. FMRP thus plays a crucial role in tuning the dendritic Kv4.2 channel density and permitting dynamic regulation of Kv4.2 during synaptic activities. We found the elevated Kv4.2 level in *fmr1* KO mice contributes to the LTP deficits (Lauterborn et al., 2007), because the Kv4 channel blocker HpTx2 dose-dependently restored LTP induction by five theta bursts (Figure 6). Given that hippocampal CA1 neurons lacking FMRP can exhibit LTP in response to strong stimuli (ten theta bursts) (Lauterborn et al., 2007), Kv4.2 suppression by FMRP appears to be important for maintaining these neurons within the dynamic range for synaptic plasticity. Moreover, concurrent with NMDAR-induced Kv4.2 internalization and degradation (Kim et al., 2007; Lei et al., 2010), NMDAR causes derepression of Kv4.2 production by inducing FMRP dephosphorylation to restore the Kv4.2 level within 20 min (Figure 7), so as to terminate the positive feedback regulation mediated by Kv4.2 downregulation.

NMDAR-Induced Upregulation of Kv4.2 Production

Whereas chemical LTP causes Kv4.2 internalization and redistribution (Kim et al., 2007) and NMDAR activation causes significant reduction of Kv4.2 channels in a reversible manner (Lei et al., 2010), our finding of elevated Kv4.2 levels due to NMDA treatment in the presence of calpain inhibitors, taken together with the luciferase assay showing NMDAR-induced upregulation of translation associated with Kv4.2-3′UTR, strongly suggests that NMDAR activation causes increased production of Kv4.2. Because new protein synthesis is clearly required for long-lasting activity-dependent changes in synaptic transmission, the manner by which neuronal activity engages the translational machinery is key to our understanding of long-term information storage. In addition to the rapid and bidirectional remodeling of synaptic NMDAR subunit composition by A-type K^+ channel activity (Jung et al., 2008), the activity-dependent regulation of Kv4.2 expression uncovered in our study provides a mechanism for rapid recovery of Kv4.2 after NMDAR-induced degradation. Whereas immediate downregulation of Kv4.2 upon NMDAR activation corresponds to positive feedback regulation important for synaptic plasticity, NMDAR-induced upregulation of Kv4.2 provides a means for negative feedback regulation for homeostasis.

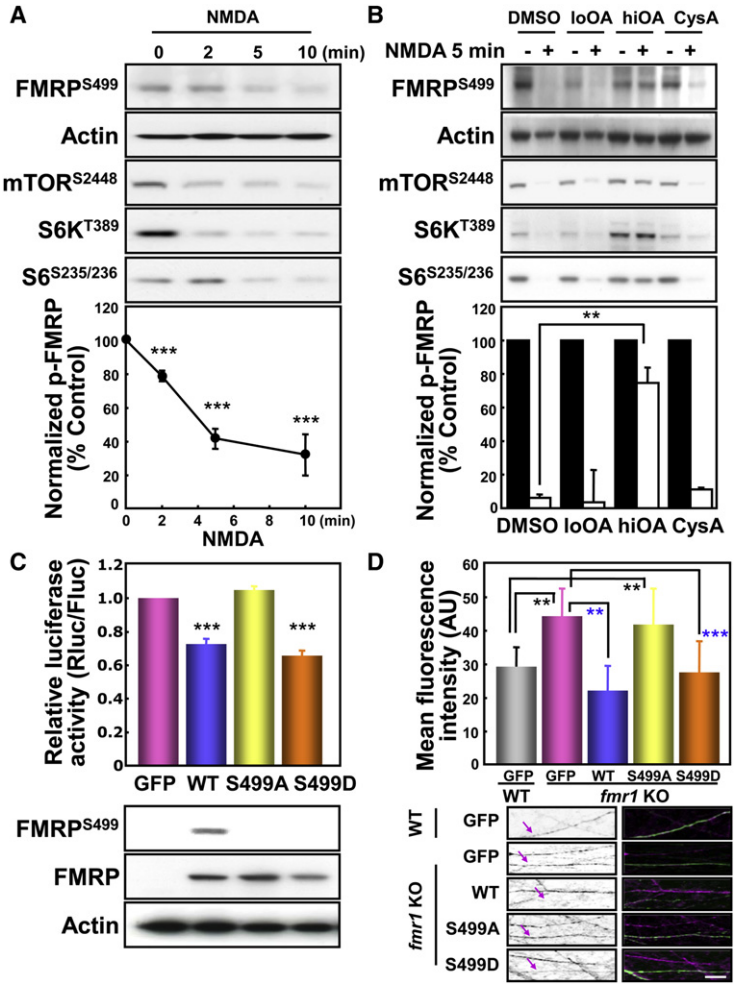

Figure 8. NMDAR Induces FMRP Dephosphorylation, which Turns Off FMRP Suppression of Kv4.2 mRNA

(A) Top: mouse hippocampal neurons (DIV14–21) were treated with 100 μM NMDA for indicated time (0, 2, 5, or 10 min). Cell lysates were immunoblotted with antibody against phospho-FMRP, actin, phospho-mTOR, phospho-S6K, or phospho-S6. Bottom: phospho-FMRP levels normalized with actin levels (% control to not-treated cells, mean ± SD; n = 4, ***p < 0.001 as compared with not-treated cells, Student's paired t test).

(B) Top: mouse hippocampal neurons (DIV14–21) were treated with 100 μM NMDA for 0 or 5 min in the presence of DMSO, 20 nM okadaic acid (loOA), 1 μM okadaic acid (hiOA), or 10 μM cyclosporine A (CysA). Cell lysates were immunoblotted with antibody against phospho-FMRP, actin, phospho-mTOR, phospho-S6K, or phospho-S6. Bottom: phospho-FMRP levels normalized with actin levels (% control to each not-treated cells, mean ± SD; n = 3, **p < 0.01 as compared with DMSO pretreated cells, Student's paired t test).

(C) Top: *Renilla* luciferase activity normalized with firefly luciferase activity (Rluc/Fluc) in HEK293 cells after transfection with GFP or GFP-tagged FMRP (WT, S499A, or S499D) (GFP-transfected cells were normalized as 1, mean ± SD; n = 4, ***p < 0.001 as compared with GFP-transfected cells, Student's paired t test). Bottom: cell lysates were immunoblotted with antibody against phospho-FMRP, FMRP, or actin. Transfected GFP-FMRPs are only shown in blot.

(D) Top: mean fluorescence intensity of surface Kv4.2 in dendrites (50–150 μm from soma) of hippocampal neurons (DIV14) from WT or *fmr1* KO mice after transfection with GFP or GFP-tagged FMRP (WT, S499A, or S499D) (mean ± SD; n = 8 dendrites for WT (GFP), KO (GFP), and KO (FMRP-WT), n = 9 dendrites for KO (FMRP-S499A) and KO (FMRP-S499D), **p < 0.01, ***p < 0.001 as compared with WT-GFP (black) or KO-GFP (blue), Student's unpaired t test). Bottom: Kv4.2 surface staining (black in single images [left]; magenta in merged images [right]) of hippocampal neurons (DIV14) from WT or *fmr1* KO mice, as described in Supplemental Experimental Procedures, after transfection with GFP or GFP-tagged FMRP (WT, S499A, or S499D) (green); scale bar represents 5 μm. See Figure S7 for rapamycin-induced FMRP dephosphorylation and Kv4.2 upregulation, and Figure S8 for the block of NMDA-induced FMRP dephosphorylation by PP1 inhibitors.

Both metabotropic and ionotropic glutamate receptors are known to regulate local protein translation. With a requirement of local protein synthesis for mGluR-dependent LTP and LTD, mGluR activation rapidly increases dendritic local protein synthesis (Sutton and Schuman, 2005). As to NMDAR-mediated translational regulation, NMDA treatment initially causes repression of overall protein synthesis (within 5 min), followed with preferential translation of specific targets such as CaMKIIα (Scheetz et al., 2000). In this study, we show that NMDAR signaling affects translation associated with Kv4.2-3′UTR and causes upregulation of Kv4.2 in an FMRP-dependent manner.

Several studies have linked FMRP to NMDAR signaling, including dynamic dendritic FMRP localization in response to visual experience (Gabel et al., 2004a), accumulation of the mRNA encoding Arc/Arg3.1, a target of FMRP, in regions of activated synapses (Steward and Worley, 2001), and NMDA-induced total protein synthesis in synaptosomes (Muddashetty et al., 2007). We found that Kv4.2 upregulation by NMDAR is due to NMDAR-induced dephosphorylation of FMRP for derepression of Kv4.2. It remains to be determined whether other transcripts besides Kv4.2 mRNA are regulated by NMDAR via the same signaling pathway.

Relief of FMRP Suppression of Kv4.2 via FMRP Dephosphorylation

Dephosphorylation of FMRP may lead to the release of polysomes from the stalled state (Ceman et al., 2003). Activation of Group1-mGluR causes rapid FMRP dephosphorylation through PP2A activation, associated with a burst of translation of FMRP targets in hippocampal neurons (Narayanan et al., 2007). Here, we show that NMDAR activation leads to rapid dephosphorylation of FMRP in a process dependent on PP1 but not PP2B, consistent with previous findings of NMDAR activation of PP1 in hippocampal neurons (Chung et al., 2009). We further asked whether NMDAR-induced upregulation of Kv4.2 might involve FMRP dephosphorylation, by testing FMRP mutants (S499A or S499D). The S499A mutation abolishes the ability of FMRP to suppress Kv4.2-3′UTR-dependent translation in luciferase assay as well as surface Kv4.2 levels, whereas the S499D mutation preserves the functions of FMRP (Figure 8). Our study thus

provides evidence for a role of the FMRP phosphorylation status on FMRP regulation of its target mRNA.

Potential Involvement of Potassium Channels in Neurological Diseases and Mental Disorders

Several reports link alterations in potassium channel expression with neurological and mental disorders. Alteration of Kv4.2 levels may be related with epilepsy and perhaps also Alzheimer's disease (Birnbaum et al., 2004). The Kv4 channel β subunits DPP6 and DPP10 are implicated in autism susceptibility (Marshall et al., 2008) and the *KCND2* gene coding for Kv4.2 is near rearrangement breakpoints of unrelated autism patients (Scherer et al., 2003). FMRP is crucial for maintaining Kv3.1b tonotopicity and its upregulation by acoustic stimulation (Strumbos et al., 2010), and mutations in *KCNC3* are responsible for spinocerebellar ataxia (SCA) in two families (Waters et al., 2006). FMRP may also control gating of the Na^+-activated K^+ channel Slack by protein-protein interaction (Brown et al., 2010). Our study showing dysregulation of Kv4.2 on hippocampal neuronal dendrites and inability of NMDAR to upregulate Kv4.2 production in *fmr1* KO mice indicates that an imbalance in the spatial and temporal regulation of Kv4.2 likely affects synaptic plasticity, and may contribute to impairments of neuronal signaling in FXS.

EXPERIMENTAL PROCEDURES

Animal Use

C57BL6/J, FVB.129P2-*Pde6b*$^+$ *Tyr*$^{c\text{-}ch}$/AntJ (control mice for *fmr1* KO), FVB.129P2-*Fmr1*^{tm1Cgr}/J (*fmr1* KO) were from the Jackson Laboratory and Kv4.2 KO mice were kindly provided by Dr. Tom Schwarz and Dr. Jeanne M. Nerbonne. The use and care of animals in this study follows the guidelines of the UCSF Institutional Animal Care and Use Committee.

Cell Cultures and Transfection

Hippocampal neurons isolated from embryonic day 17 mouse brains were plated at a density of 1–3 × 10^5 cells/well as described previously (Fu et al., 2007). HEK293 cells were maintained in Dulbecco's modified Eagle medium (DMEM) supplemented with 10% fetal bovine serum (FBS), 110 μg/ml sodium pyruvate, and 2 mM L-glutamine. Cells were kept at 37°C in a humidified CO_2-controlled (5%) incubator and were transfected using Lipofectamine 2000.

Immunostaining

Hippocampal neurons grown on coverslips were immunostained with or without prior transfection. Cells were washed with phosphate-buffered saline (PBS), fixed in 4% formaldehyde, and incubated in blocking buffer (1% goat serum in PBS containing 0.1% Triton X-100), then incubated with primary antibody for 4 hr followed with secondary antibody for 1 hr at room temperature, and examined under a Leica TCS SP2 confocal microscope (Leica Microsystems, Bannockburn, IL).

Western Blot Analysis

Proteins denatured by heating for 15 min at 60°C in Laemmli sample buffer (Laemmli, 1970) were separated by SDS-PAGE and transferred to nitrocellulose membranes. After blocking in TTBS buffer (10 mM Tris-HCl, pH 7.5, 150 mM NaCl, 0.05% Tween 20, and 5% skim milk powder), the membranes were incubated with primary antibody overnight at 4°C and then with horseradish peroxidase (HRP)-secondary antibody for 1 hr at room temperature. Detection was performed using an enhanced chemiluminescence (ECL) kit and Hyperfilm MP, and quantified using a Fuji BAS-2000 image analyzer.

Treatment of NMDA in Primary Hippocampal Culture

Hippocampal neurons (DIV14–21) were incubated with neurobasal medium for 5 min (control) or with neurobasal medium containing 100 μM NMDA for 5 min at 37°C, washed twice with neurobasal medium and then maintained in the medium for 15 min or time indicated in results.

Miscellaneous

Additional information on materials, antibodies, DNA constructs, protein purification, slice in Situ hybridization, FISH in cultured hippocampal neurons, tracking mRNA using MS2 system, live imaging using Dendra-Kv4.2, immunoprecipitation of FMRP in brain lysates, quantitative RT-PCR, biotinylated RNA and protein binding assay, immunohistochemistry, surface biotinylation, surface staining, in vitro translation assay, luciferase reporter assay and LTP experiment are described in Supplemental Experimental Procedures.

SUPPLEMENTAL INFORMATION

Supplemental Information includes Supplemental Experimental Procedures and eight figures and can be found with this article online at doi:10.1016/j.neuron.2011.09.033.

ACKNOWLEDGMENTS

We thank Drs. Tom Schwarz and Jeanne M. Nerbonne for kindly providing Kv4.2 KO mice, Dr. Lynn Regan for kindly providing mouse full-length FMRP construct, Dr. Stephanie Ceman for kindly providing GFP-FMRP constructs, Dr. Marc I. Diamond for kindly providing pcDNA3-mouse H1d construct, Dr. Seung Key Jang for sharing MS2-GFP-NLS and MS2BS(6X) constructs, and Dr. Philippe Mourrain and Gemini Skariah for the help and support they provided for the in situ hybridization procedure. We also thank Denan Wang for maintaining mouse lines, Marena Tynan-La Fontaine for genotyping, Dr. Sila Konur for help with imaging and for critical reading of the manuscript and Dr. Desiree Thayer for critical reading of the manuscript and many helpful discussions. This work was supported by the National Institute of Mental Health (L.Y.J.). Y.N.J. and L.Y.J. are investigators of the Howard Hughes Medical Institute.

Accepted: September 2, 2011
Published: November 16, 2011

REFERENCES

Antar, L.N., and Bassell, G.J. (2003). Sunrise at the synapse: the FMRP mRNP shaping the synaptic interface. Neuron *37*, 555–558.

Antar, L.N., Afroz, R., Dictenberg, J.B., Carroll, R.C., and Bassell, G.J. (2004). Metabotropic glutamate receptor activation regulates fragile x mental retardation protein and FMR1 mRNA localization differentially in dendrites and at synapses. J. Neurosci. *24*, 2648–2655.

Bagni, C., and Greenough, W.T. (2005). From mRNP trafficking to spine dysmorphogenesis: the roots of fragile X syndrome. Nat. Rev. Neurosci. *6*, 376–387.

Bassell, G.J., and Warren, S.T. (2008). Fragile X syndrome: loss of local mRNA regulation alters synaptic development and function. Neuron *60*, 201–214.

Bear, M.F., Huber, K.M., and Warren, S.T. (2004). The mGluR theory of fragile X mental retardation. Trends Neurosci. *27*, 370–377.

Birnbaum, S.G., Varga, A.W., Yuan, L.L., Anderson, A.E., Sweatt, J.D., and Schrader, L.A. (2004). Structure and function of Kv4-family transient potassium channels. Physiol. Rev. *84*, 803–833.

Brown, M.R., Kronengold, J., Gazula, V.R., Chen, Y., Strumbos, J.G., Sigworth, F.J., Navaratnam, D., and Kaczmarek, L.K. (2010). Fragile X mental retardation protein controls gating of the sodium-activated potassium channel Slack. Nat. Neurosci. *13*, 819–821.

Ceman, S., O'Donnell, W.T., Reed, M., Patton, S., Pohl, J., and Warren, S.T. (2003). Phosphorylation influences the translation state of FMRP-associated polyribosomes. Hum. Mol. Genet. *12*, 3295–3305.

Chen, L., Yun, S.W., Seto, J., Liu, W., and Toth, M. (2003). The fragile X mental retardation protein binds and regulates a novel class of mRNAs containing U rich target sequences. Neuroscience *120*, 1005–1017.

Chen, X., Yuan, L.L., Zhao, C., Birnbaum, S.G., Frick, A., Jung, W.E., Schwarz, T.L., Sweatt, J.D., and Johnston, D. (2006). Deletion of Kv4.2 gene eliminates dendritic A-type K+ current and enhances induction of long-term potentiation in hippocampal CA1 pyramidal neurons. J. Neurosci. *26*, 12143–12151.

Chung, H.J., Qian, X., Ehlers, M., Jan, Y.N., and Jan, L.Y. (2009). Neuronal activity regulates phosphorylation-dependent surface delivery of G protein-activated inwardly rectifying potassium channels. Proc. Natl. Acad. Sci. USA *106*, 629–634.

Comery, T.A., Harris, J.B., Willems, P.J., Oostra, B.A., Irwin, S.A., Weiler, I.J., and Greenough, W.T. (1997). Abnormal dendritic spines in fragile X knockout mice: maturation and pruning deficits. Proc. Natl. Acad. Sci. USA *94*, 5401–5404.

Dictenberg, J.B., Swanger, S.A., Antar, L.N., Singer, R.H., and Bassell, G.J. (2008). A direct role for FMRP in activity-dependent dendritic mRNA transport links filopodial-spine morphogenesis to fragile X syndrome. Dev. Cell *14*, 926–939.

Edbauer, D., Neilson, J.R., Foster, K.A., Wang, C.F., Seeburg, D.P., Batterton, M.N., Tada, T., Dolan, B.M., Sharp, P.A., and Sheng, M. (2010). Regulation of synaptic structure and function by FMRP-associated microRNAs miR-125b and miR-132. Neuron *65*, 373–384.

Fu, W.Y., Chen, Y., Sahin, M., Zhao, X.S., Shi, L., Bikoff, J.B., Lai, K.O., Yung, W.H., Fu, A.K., Greenberg, M.E., and Ip, N.Y. (2007). Cdk5 regulates EphA4-mediated dendritic spine retraction through an ephexin1-dependent mechanism. Nat. Neurosci. *10*, 67–76.

Fusco, D., Accornero, N., Lavoie, B., Shenoy, S.M., Blanchard, J.M., Singer, R.H., and Bertrand, E. (2003). Single mRNA molecules demonstrate probabilistic movement in living mammalian cells. Curr. Biol. *13*, 161–167.

Gabel, L.A., Won, S., Kawai, H., McKinney, M., Tartakoff, A.M., and Fallon, J.R. (2004a). Visual experience regulates transient expression and dendritic localization of fragile X mental retardation protein. J. Neurosci. *24*, 10579–10583.

Gabel, L.A., Won, S., Kawai, H., McKinney, M., Tartakoff, A.M., and Fallon, J.R. (2004b). Visual experience regulates transient expression and dendritic localization of fragile X mental retardation protein. J. Neurosci. *24*, 10579–10583.

Greenough, W.T., Klintsova, A.Y., Irwin, S.A., Galvez, R., Bates, K.E., and Weiler, I.J. (2001). Synaptic regulation of protein synthesis and the fragile X protein. Proc. Natl. Acad. Sci. USA *98*, 7101–7106.

Gross, C., Yao, X., Pong, D.L., Jeromin, A., and Bassell, G.J. (2011). Fragile X mental retardation protein regulates protein expression and mRNA translation of the potassium channel Kv4.2. J. Neurosci. *31*, 5693–5698.

Hinton, V.J., Brown, W.T., Wisniewski, K., and Rudelli, R.D. (1991). Analysis of neocortex in three males with the fragile X syndrome. Am. J. Med. Genet. *41*, 289–294.

Irwin, S.A., Patel, B., Idupulapati, M., Harris, J.B., Crisostomo, R.A., Larsen, B.P., Kooy, F., Willems, P.J., Cras, P., Kozlowski, P.B., et al. (2001). Abnormal dendritic spine characteristics in the temporal and visual cortices of patients with fragile-X syndrome: a quantitative examination. Am. J. Med. Genet. *98*, 161–167.

Jo, A., Nam, Y.J., Oh, J.Y., Cheon, H.S., Jeromin, A., Lee, J.A., and Kim, H.K. (2010). Dendritic localization and a cis-acting dendritic targeting element of Kv4.2 mRNA. BMB Rep. *43*, 677–682.

Jung, S.C., Kim, J., and Hoffman, D.A. (2008). Rapid, bidirectional remodeling of synaptic NMDA receptor subunit composition by A-type K+ channel activity in hippocampal CA1 pyramidal neurons. Neuron *60*, 657–671.

Kelleher, R.J., 3rd, Govindarajan, A., and Tonegawa, S. (2004). Translational regulatory mechanisms in persistent forms of synaptic plasticity. Neuron *44*, 59–73.

Kiebler, M.A., and Bassell, G.J. (2006). Neuronal RNA granules: movers and makers. Neuron *51*, 685–690.

Kim, J., and Hoffman, D.A. (2008). Potassium channels: newly found players in synaptic plasticity. Neuroscientist *14*, 276–286.

Kim, J., Jung, S.C., Clemens, A.M., Petralia, R.S., and Hoffman, D.A. (2007). Regulation of dendritic excitability by activity-dependent trafficking of the A-type K+ channel subunit Kv4.2 in hippocampal neurons. Neuron *54*, 933–947.

Laemmli, U.K. (1970). Cleavage of structural proteins during the assembly of the head of bacteriophage T4. Nature *227*, 680–685.

Lauterborn, J.C., Rex, C.S., Kramár, E., Chen, L.Y., Pandyarajan, V., Lynch, G., and Gall, C.M. (2007). Brain-derived neurotrophic factor rescues synaptic plasticity in a mouse model of fragile X syndrome. J. Neurosci. *27*, 10685–10694.

Lei, Z., Deng, P., and Xu, Z.C. (2008). Regulation of Kv4.2 channels by glutamate in cultured hippocampal neurons. J. Neurochem. *106*, 182–192.

Lei, Z., Deng, P., Li, Y., and Xu, Z.C. (2010). Downregulation of Kv4.2 channels mediated by NR2B-containing NMDA receptors in cultured hippocampal neurons. Neuroscience *165*, 350–362.

Marshall, C.R., Noor, A., Vincent, J.B., Lionel, A.C., Feuk, L., Skaug, J., Shago, M., Moessner, R., Pinto, D., Ren, Y., et al. (2008). Structural variation of chromosomes in autism spectrum disorder. Am. J. Hum. Genet. *82*, 477–488.

Menegola, M., and Trimmer, J.S. (2006). Unanticipated region- and cell-specific downregulation of individual KChIP auxiliary subunit isotypes in Kv4.2 knock-out mouse brain. J. Neurosci. *26*, 12137–12142.

Muddashetty, R.S., Kelić, S., Gross, C., Xu, M., and Bassell, G.J. (2007). Dysregulated metabotropic glutamate receptor-dependent translation of AMPA receptor and postsynaptic density-95 mRNAs at synapses in a mouse model of fragile X syndrome. J. Neurosci. *27*, 5338–5348.

Narayanan, U., Nalavadi, V., Nakamoto, M., Pallas, D.C., Ceman, S., Bassell, G.J., and Warren, S.T. (2007). FMRP phosphorylation reveals an immediate-early signaling pathway triggered by group I mGluR and mediated by PP2A. J. Neurosci. *27*, 14349–14357.

Narayanan, U., Nalavadi, V., Nakamoto, M., Thomas, G., Ceman, S., Bassell, G.J., and Warren, S.T. (2008). S6K1 phosphorylates and regulates fragile X mental retardation protein (FMRP) with the neuronal protein synthesis-dependent mammalian target of rapamycin (mTOR) signaling cascade. J. Biol. Chem. *283*, 18478–18482.

Nimchinsky, E.A., Oberlander, A.M., and Svoboda, K. (2001). Abnormal development of dendritic spines in FMR1 knock-out mice. J. Neurosci. *21*, 5139–5146.

Penagarikano, O., Mulle, J.G., and Warren, S.T. (2007). The pathophysiology of fragile x syndrome. Annu. Rev. Genomics Hum. Genet. *8*, 109–129.

Pilpel, Y., Kolleker, A., Berberich, S., Ginger, M., Frick, A., Mientjes, E., Oostra, B.A., and Seeburg, P.H. (2009). Synaptic ionotropic glutamate receptors and plasticity are developmentally altered in the CA1 field of Fmr1 knockout mice. J. Physiol. *587*, 787–804.

Raab-Graham, K.F., Haddick, P.C., Jan, Y.N., and Jan, L.Y. (2006). Activity- and mTOR-dependent suppression of Kv1.1 channel mRNA translation in dendrites. Science *314*, 144–148.

Ramakers, G.M., and Storm, J.F. (2002). A postsynaptic transient K(+) current modulated by arachidonic acid regulates synaptic integration and threshold for LTP induction in hippocampal pyramidal cells. Proc. Natl. Acad. Sci. USA *99*, 10144–10149.

Sanguinetti, M.C., Johnson, J.H., Hammerland, L.G., Kelbaugh, P.R., Volkmann, R.A., Saccomano, N.A., and Mueller, A.L. (1997). Heteropodatoxins: peptides isolated from spider venom that block Kv4.2 potassium channels. Mol. Pharmacol. *51*, 491–498.

Scheetz, A.J., Nairn, A.C., and Constantine-Paton, M. (2000). NMDA receptor-mediated control of protein synthesis at developing synapses. Nat. Neurosci. *3*, 211–216.

Scherer, S.W., Cheung, J., MacDonald, J.R., Osborne, L.R., Nakabayashi, K., Herbrick, J.A., Carson, A.R., Parker-Katiraee, L., Skaug, J., Khaja, R., et al. (2003). Human chromosome 7: DNA sequence and biology. Science *300*, 767–772.

Schuman, E.M., Dynes, J.L., and Steward, O. (2006). Synaptic regulation of translation of dendritic mRNAs. J. Neurosci. *26*, 7143–7146.

Sossin, W.S., and DesGroseillers, L. (2006). Intracellular trafficking of RNA in neurons. Traffic *7*, 1581–1589.

Steward, O., and Worley, P.F. (2001). Selective targeting of newly synthesized Arc mRNA to active synapses requires NMDA receptor activation. Neuron *30*, 227–240.

Strumbos, J.G., Brown, M.R., Kronengold, J., Polley, D.B., and Kaczmarek, L.K. (2010). Fragile X mental retardation protein is required for rapid experience-dependent regulation of the potassium channel Kv3.1b. J. Neurosci. *30*, 10263–10271.

Sutton, M.A., and Schuman, E.M. (2005). Local translational control in dendrites and its role in long-term synaptic plasticity. J. Neurobiol. *64*, 116–131.

Waters, M.F., Minassian, N.A., Stevanin, G., Figueroa, K.P., Bannister, J.P., Nolte, D., Mock, A.F., Evidente, V.G., Fee, D.B., Müller, U., et al. (2006). Mutations in voltage-gated potassium channel KCNC3 cause degenerative and developmental central nervous system phenotypes. Nat. Genet. *38*, 447–451.

Zalfa, F., Giorgi, M., Primerano, B., Moro, A., Di Penta, A., Reis, S., Oostra, B., and Bagni, C. (2003). The fragile X syndrome protein FMRP associates with BC1 RNA and regulates the translation of specific mRNAs at synapses. Cell *112*, 317–327.

Zalfa, F., Eleuteri, B., Dickson, K.S., Mercaldo, V., De Rubeis, S., di Penta, A., Tabolacci, E., Chiurazzi, P., Neri, G., Grant, S.G., and Bagni, C. (2007). A new function for the fragile X mental retardation protein in regulation of PSD-95 mRNA stability. Nat. Neurosci. *10*, 578–587.